



## Original Article

## Developing an interface strength technique using the laser shock method



James A. Smith\*, Bradley C. Benefiel, Clark L. Scott

Nuclear/Reactor Engineering Department, Idaho National Laboratory, 2525 Fremont Avenue, Idaho Falls, ID, 83415-2209, USA

## ARTICLE INFO

## Article history:

Received 1 March 2022

Received in revised form

22 July 2022

Accepted 27 September 2022

Available online 25 October 2022

## Keywords:

Laser shock (LS)  
Interface strength  
Nuclear plate fuel  
Characterization  
Sensing  
Shockwaves

## ABSTRACT

Characterizing the behavior of nuclear reactor plate fuels is vital to the progression of advanced fuel systems. The states of pre- and post-irradiation plates need to be determined effectively and efficiently prior to and following irradiation. Due to the hostile post-irradiation environment, characterization must be completed remotely. Laser-based characterization techniques enable the ability to make robust measurements inside a hot-cell environment. The Laser Shock (LS) technique generates high energy shockwaves that propagate through the plate and mechanically characterizes cladding-cladding interfaces.

During an irradiation campaign, two Idaho National Laboratory (INL) fabricated MP-1 plates had a fuel breach in the cladding-cladding interface and trace amounts of fission products were released. The objective of this report is to characterize the cladding-cladding interface strengths in three plates fabricated using different fabrication processes. The goal is to assess the risk in irradiating future developmental and production fuel plates. Prior LS testing has shown weaker and more variability in bond strengths within INL MP-1 reference plates than in commercially produced vendor plates. Three fuel plates fabricated with different fabrication processes will be used to bound the bond strength threshold for plate irradiation insertion and assess the confidence of this threshold value.

© 2022 Korean Nuclear Society, Published by Elsevier Korea LLC. This is an open access article under the CC BY-NC-ND license (<http://creativecommons.org/licenses/by-nc-nd/4.0/>).

## 1. Introduction

Within the United States (U.S.) Department of Energy's (DOE's) Material Management and Minimization (M3) office, the U.S. High Performance Research Reactor (USHPRR) Project has been tasked with the development, qualification, and licensing of new fuel systems to convert five high-power research reactors and one critical assembly in the U.S. from high-enriched uranium (HEU) to low-enriched uranium (LEU) [1]. The development and selection of the U-10Mo monolithic LEU fuel system has been completed with the establishment and scale-up of the selected fabrication process involving U-10Mo foils, co-rolled with zirconium diffusion barrier interlayers, and cladding in aluminum alloy (AA) 6061 using a hot isostatic press (HIP).

Historically, the most likely root cause of fuel failure within a nuclear reactor is the separation (debond) between the enclosed fuel and cladding. The space generated by a debond produces a local rise in temperature that can initiate melting of the cladding

and ultimately fuel failure. The Laser Shock System (LSS) is designed to characterize the fuel/cladding interface in fresh and irradiated fuels [2–7]. A measure of the interface strength will enable the qualification of LEU fuel for use in research reactors, in addition to providing a method to evaluate fabrication processes.

The ability to develop new fuels for performance, safety, and nuclear safeguards applications requires the ability to characterize the reaction of nuclear fuels and materials within the reactor. Irradiated fuels are required to be studied within a high-radiation environment. The LSS provides a capability to remotely measure fuel characteristics in a robust manner within a hot-cell [3–7]. This system offers spatial resolution suitable for scanning and imaging large areas.

The MP-1 irradiation experiment was the first in a series of fuel testing campaigns aimed at achieving regulatory qualification of the U-10Mo monolithic plate-type fuel system. The objective of MP-1 was to assess the performance behavior of fuel plates fabricated by a commercial fuel fabricator and to ensure that this fuel meets the requirements of maintaining mechanical integrity, geometric stability, and behaving in a stable and predictable manner. An additional objective was to tie the commercial fabricated fuel

\* Corresponding author.

E-mail address: [james.smith@inl.gov](mailto:james.smith@inl.gov) (J.A. Smith).

performance behavior back to fuel fabricated by prototype processes developed at Idaho National Laboratory (INL) that have an established behavior. The two sets of fuel plates were fabricated and inspected to the similar fuel plate specifications; however, because two different fabricators (e.g., INL and commercial) were utilized, processes and methods were different to some extent.

The MP-1 experiment consisted of multiple mini-plate capsules distributed within INL's Advanced Test Reactor (ATR) core. Each capsule contains eight mini-plates that were either fueled or 'dummy' plates. During the irradiation cycle, trace fission products were detected in the Real Time Stack Monitor (RTSM) and the Primary Coolant System (PCS). Two of the capsules revealed the presence of fission product radionuclides characteristic of breached fuel plates. These capsules had both commercially and INL-fabricated plates. During capsule disassembly and visual examination in the hot-cell, two failed fuel plates were identified. The failures were indicated visually by a separation of the cladding-cladding bond-line on the edge of the plates and edge-staining potentially caused by the release of solid fission products. The failed plates were identified as INL-fabricated plates. None of the commercial plates had similar indications of cladding-cladding bond-line failure, as determined by visual examination. Delamination of the cladding-cladding bond-line was not anticipated. Prior to these plate failures, interface characterization was focused on the fuel-cladding interface [3–5]. This incident quickly changed the program's short-term focus to the cladding-cladding interface.

Since the cladding failures were limited to INL plates, there is concern that the INL fabrication process may have produced fuel plates with lower cladding-cladding interface strengths than the commercial plates. The root cause of the failure needs to be determined to ensure that the industrial fabrication process is immune to the cause of the INL cladding failures. The focus of the Laser Shock (LS) characterization system has been in determining bond strength for cladding-fuel interfaces. To determine if there is a systematic cladding-cladding bond strength difference between the INL and commercial fabrication processes, a modification to the fuel-cladding technique will be required to enable the LS characterization system to make reliable measurements. The typical cladding-cladding interface strength is much stronger than the dissimilar material fuel-cladding interface. The LS technique, in general, cannot reliably break a typical cladding-cladding bond with a single interrogation. It is necessary to develop a modified measurement technique for the cladding-cladding interface.

The main objective of this work is to compare interface strengths in cladding-cladding regions between MP-1 fuel plates fabricated with different processes and by different fabricators. The interface strengths of the plates will be mapped/characterized, which will capture variations inherent in the plate fabrication process. The bond strength differences between INL's Reduced Enrichment for Research and Test Reactors (RERTR) and MP-1 plates, as well as differences between the INL- and vendor-fabricated plates, are a focus of this work. The mapping of the variation as a function of location in a plate will determine if excess material obtained by punching the fuel plates out of a HIPed frame can predict fuel plate interface strength.

The fundamental principles of the LSS and a description of the system will be presented. The three fuel plate specimens will be used to compare fabrication processes, as well as the supplemental results from prior characterization testing. In order to characterize the cladding-cladding samples, the LS technique needed to be modified. This new characterization method will be described. The results from the LS cladding-cladding testing will be reviewed. The salient results will be summarized in the conclusion.

## 1.1. LS technique review

The LS technique uses large amplitude shockwaves generated by a laser that characterizes mechanical interfaces, such as thin films [8–11], adhesive layers [12,13], metal-to-ceramic bonds [14], and currently, fuel/cladding bond-lines [3–5]. The laser creates a shockwave that travels as a compression wave in the material to the unconstrained reflecting surface, which then gets reflected back toward the generation surface as a tensile wave. The reflected tensile shockwave is the mechanical mechanism that produces interface failure.

The LSS has been used to test fuel plates made from a monolithic fuel meat consisting of a U–Mo alloy foil (typically 0.2–0.4 mm thick) and cladding with Al-6061, as displayed in Fig. 1. The total thickness of the plate can vary from 1.3 to 1.6 mm. The bond-line between the fuel foil and the aluminum (Al) plate must establish the necessary geometric stability to be eligible for qualification by the U.S. Nuclear Regulatory Commission (NRC) and DOE for test reactor use. LS testing can be performed at numerous positions on a specimen. For fuel-cladding testing, the interface strength is determined by increasing the shock energy until debonding is detected by laser-ultrasonic-testing (LUT) imaging. The normal configuration of the LSS comprises a shock laser and two subsystems: (1) the LUT C-scan imaging subsystem that detects interface failure; and (2) the surface velocity measurement subsystem that quantifies bond strength. For the cladding-cladding testing, the surface velocity measurement is not practical to use without advanced material modeling efforts. The interrogated cladding material will be plastically deformed during the measurement process. The large change in the Al properties due to the plastic deformation confounds the interpretation of the surface velocity measurements. The LUT imaging subsystem and shock laser utilized in this work are displayed in Fig. 2.

The LUT subsystem consists of a 10 ns pulsed laser source and an ultrasonic testing (UT) system. The 10 ns pulse laser, or generation laser, creates a short ultrasonic pulse that characterizes the fuel plate. UT detection consists of a longer 50  $\mu$ s pulse laser and a photorefractive interferometer to monitor the surface displacements caused by laser-generated ultrasound. The LUT subsystem is shown at the top of Fig. 2. The shock-generation laser consists of a high energy and short pulse laser (e.g., 2.7 J, 10 ns pulse). The laser pulse coming from the shock laser creates a shockwave that is boosted by placing constraining layers on the specimen surface.

Large-core fiber optics are used to transmit the detection laser light through a pathway converter box and on to the fuel plate depending on the desired measurement, velocity, or LUT. Optical fibers can efficiently transport light because the fibers are flexible and easier to route and align than bulk optics. However, energy in the shock laser pulse is too large to be injected through a fiber and must be delivered via free space and bulk optics. Hot-cell applications require sacrificial fibers to be used because fibers ultimately darken from the effects of radiation. The converter box shown in

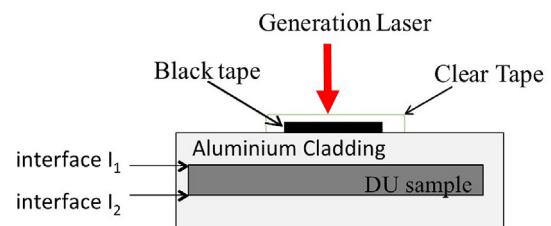
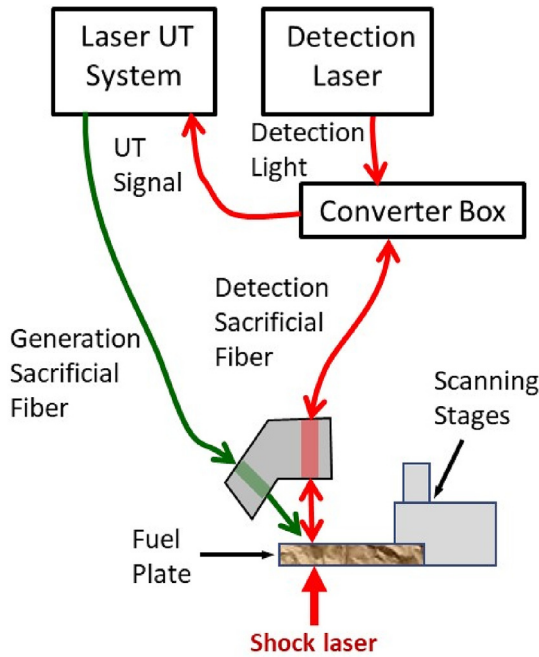


Fig. 1. A schematic of a plate fuel specimen (DU-Mo), geometry, and a plasma-constraining mechanism to generate larger shockwaves.



**Fig. 2.** For this work, the LSS consists of the shock laser and LUT subsystem. The converter box is used to allow the sacrificial fibers to go into the hot-cell as they need to be replaced periodically.

Fig. 2 also permits the use of sacrificial fibers to transmit light into the hot-cell and provide a mechanism to efficiently replace the fibers periodically. The UT detection light is transported to the optical head using the detection sacrificial optical fiber. The light exiting the fiber is collimated and then focused on the plate's surface using bulk optics. The back-reflected light from the specimen's surface is routed to the UT detector in the LUT subsystem via the converter box.

The generation light in the LUT system is also delivered to the optical head via the optical fiber. The generation light is focused on the same spot as the UT detection light, which generates a small amplitude ultrasonic signal, while the UT detection light monitors the surface displacements of the ultrasound traveling and reverberating through the thickness of the plate at that interrogation spot. The LUT system performs the UT C-scan imaging of the plate to detect interface debonding.

The high-power light pulse from the shock laser generates the large amplitude shockwaves that stress the interfaces in the fuel. To increase the efficacy of the optical-to-mechanical conversion, the plate's surface is layered with optically absorbent black tape, which is overlaid with a clear constraining tape [3–5], as shown in Fig. 1. The high energy laser produces an explosive plasma when it reaches the black tape. The rapidly expanding plasma is constrained by the tough high-temperature clear tape and a magnified shockwave is created by generating large amplitude surface displacements that cause significant plastic deformation.

The source size of the resulting shockwave is approximately the laser spot size generating the plasma from the black tape. For optimum performance, the laser spot size should be approximately two times the sample thickness for the resulting shockwave propagation to be considered one-dimensional (1-D). Assuming 1-D approximation, the shear stresses are neglected, and the shockwave is presumed to be completely compressive. The propagating shockwave is reflected by the far surface of the plate and transformed into a tensile wave. The resulting tensile stresses can debond interfaces. Fuel-cladding bond strength is measured by

incrementing the shock laser energy by small steps until a debond is indicated by the LUT system. For our application, there is not enough unobstructive cladding-cladding space to interrogate a fresh location at each laser energy.

The above procedure for interface strength measurement works well for dissimilar interfaces, such as fuel-cladding, because the failure threshold is below the maximum shockwave amplitude that can be achieved, and the resulting shockwaves are mostly elastic in nature. The typical interface strength for cladding-cladding is much stronger than fuel-cladding interface strength. It is infrequent when a cladding-cladding interface is debonded with a single full power LS interrogation. Because the shockwave amplitudes are at maximum energy for cladding-cladding bonds, there is a significant amount of plastic deformation and changes in microstructure within the Al cladding. Given these physical variations to the plate material, another interface characterization technique had to be developed for cladding-cladding interfaces.

### 1.2. Cladding-cladding characterization

As stated previously, cladding-cladding characterization has not been a focus for LS characterization. Prior to the MP-1 plates, the LS program has not been able to reliably debond typical cladding-cladding interfaces. Interface characterization requires the ability to break interfaces, ideally without structurally changing or yielding the materials. Fabrication parameters were changed between the fabrication of the RERTR and MP-1 fuel plates. Significant changes were made within the fabrication process, as well as in fuel plate thickness. The bond strength differences between INL's RERTR and MP-1 plates, as well as differences between the INL and vendor plates, are goals of this work.

A robust clad-clad interface takes an enormous amount of energy to yield the material around the interface and cause enough plastic deformation to fracture and fail the interface. The LS technique imparts a massive amount of energy in the form of a shockwave in the Al cladding. This is apparent because of the visible craters left on the generation side and the dimples left on the reflection side of the plate, as seen in Fig. 3. The material yielding is throughout the thickness of the plate, as revealed in Fig. 3(b). Despite this amount of plastic deformation, historical testing has shown that a single shockwave still cannot reliably debond a typical cladding-cladding interface. The yielding and plastic deformation of the Al dissipates a significant amount of energy via several mechanisms within a short distance (<0.10 mm). This energy dissipation is currently the Achilles heel of the LS technique. Energy dissipation also limits the tensile force that can be applied to the interface. Although we can calculate the amount of energy that reaches the reflection side based on surface velocity, the reflected tensile shockwave loses energy as the shockwave propagates back toward the interface. Thus, plates with different interface depths will be difficult to compare without advanced (e.g., non-elastic) modeling as the shockwave energy at the interface will be different. A direct comparison can be made for plates with the same geometry and material composition.

Because it is atypical for the LSS to break cladding-cladding bonds on the first shot at maximum power and the cladding is severely plastically deformed, surface velocity measurements are not a straightforward indicator of cladding-cladding bond strength. This is, in part, due to geometric effects caused by an existing dimple affecting the 1-D assumption, microstructure changes, and optical-to-mechanical transfer function degradation in the constraining system. The reported bond strength for cladding-cladding measurements presented in this report will be based on the presence or absence of interface failure. The bond strength figure of merit for cladding-cladding measurements that is reported will be

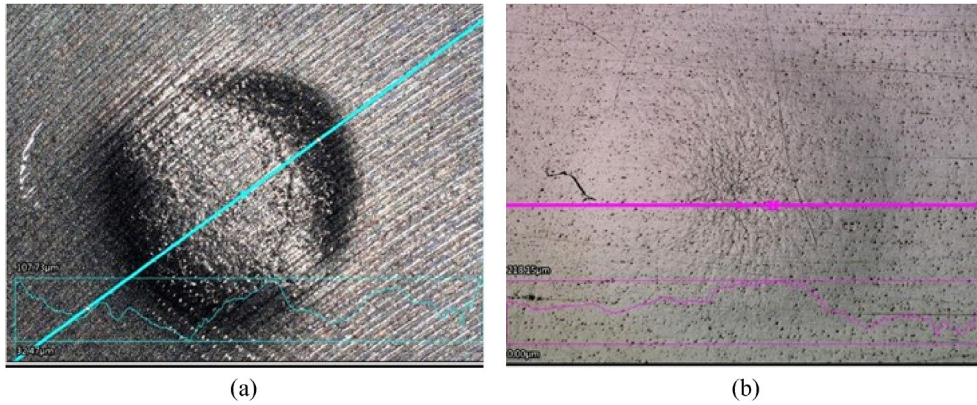


**Fig. 3.** The surface of the fuel plate is plastically deformed from the LS on generation and reflection sides: (a) generation side deformation; and (b) reflected side deformation. The reflected surface can protrude by as much as 0.5 mm.

based on the presence or absence of interface failure.

A quasi-quantitative technique has been developed for the cladding-cladding interfaces. The quasi-quantitative bond strength figure of merit involves hitting a specimen at least once with a maximum energy shock laser pulse ( $\approx 2.7$  J), and then checking to see if the interface failed. If the interface is still intact, the specimen is shocked again. This process is repeated until the interface breaks, or the specimen has been shocked at the same location three times, whichever comes first. After three full power shots, the surface crater created by the laser shocks becomes too deep for the containment system to be effective. The interface strength measurement is quasi-quantitative by counting the number of full power shots (e.g., LS shot number) it takes to break the interface up to three shots.

To identify failures in the interfaces being tested, the LSS has a separate UT imaging subsystem. The LUT C-scan subsystem detects and images interface failures caused by the LSS. LUT images are created pre- and post-LSS interrogation, as shown in Fig. 4. The C-scan images monitor the occurrence of debonds after each interrogation shot and are used to determine the size and depth location of the debond. LUT imaging is achieved on the plate’s reflecting

surface, as shown previously in Fig. 2, and is analogous to a traditional ultrasonic C-scan.

## 2. Materials

The M3 program supplied a number of historical and current fuel plates, which consist of a combination of INL and commercially fabricated plates. The INL MP-1 reference plates were fabricated as outlined in the summary report [15]. The other INL-fabricated plates followed a similar fabrication process [15]. The vendor plates were fabricated according to the outline in the vendor scope of work (SOW) [16]. The nominal sizes of the MP-1 fuel plates are 25.4 mm  $\times$  101.6 mm  $\times$  1.24 mm.

The following main fuel plates were tested:

- 
- 67-1 INL-fabricated blank frame (no fuel foil) using the RERTR-12 process [17].
  - A1C168 vendor-fabricated thin fuel plate
  - 108-3 INL-fabricated reference thick foil fuel plate.
- 

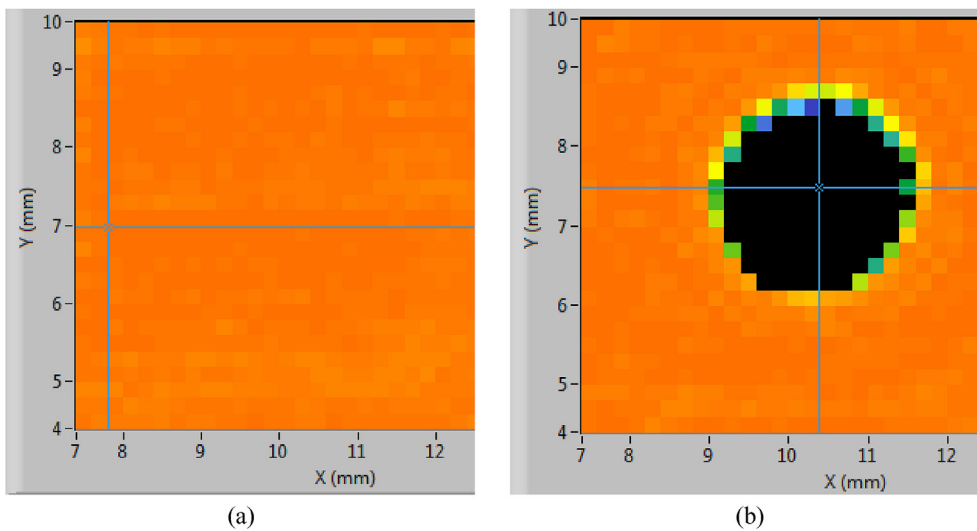


**Fig. 4.** LUT C-scan images of a fuel plate are shown.(a) Pre-scan baseline image and (b) post-LS interrogation showing a debond.



The blank 67-1 frame was fabricated as a nominally thicker plate (i.e., 1.42 mm). The 67-1 plate was machined down to the nominal MP-1 thickness of 1.24 mm so that the cladding-cladding interface was along the centerline of the plate. The A1C168 vendor plate is fabricated with the bond-line along the center of the plate. All vendor plates are fabricated with the interface depth coinciding with the plate's centerline without regard to the fuel foil thickness. The INL reference plate was fabricated with the bond-line off-center (i.e., 0.965 mm) from the backside of the plate, as shown in Fig. 5. The front side of the plate has the plate number or frame number stamped on it.

### 3. Methods

The number of interrogations it takes to cause interface failure is reported as the LS shot number. The LUT C-scan of the LS interrogation shot point determines the status of the interface. Since only up to three LS shots can be effectively executed at one location, the resulting 'quantization' error is relatively large. Despite the quantization limitations, the resulting data will be shown to be surprisingly useful in characterizing bond strength throughout the plate.

Due to the limited number of test samples and interrogation locations, supporting data from prior characterization efforts [18] are also utilized in this report to confirm possible trends. The supporting data has been obtained from intact fuel plates, shear drops from INL HIPed frames, and punch drops from the vendor HIPed frames. Shear and punch drops are generated from excess HIPed fuel frame material by cutting out the fuel plates [15,16].

INL plate 108-3 is a thick foil plate and cannot be directly compared to the 67-1 and A1C168 plates since the location of the bond-line is not along the center of the plate, as observed in Fig. 5. The data from plate 108-3 can be compared to previous data taken on MP-1 thick foil plates fabricated using the INL MP-1 process. Previous data for MP-1 fuel plate A2B104 will be compared to INL plate 108-3.

### 4. Results

This section will present the results from testing INL samples 108-3 and 67-1, as well as vendor sample A1C168. These results will be supplemented with the appropriate prior results [18] to help understand trends in the data. The tabular results will display the following information:

- specimen
- shot point interrogation location
- laser energy
- maximum measured back surface velocity for the first full energy shot
- measurement of the material property characteristic, Hugoniot Elastic Limit (HEL) [6], for the first full energy shot
- LS shot number for which the interface failed through the semi-quantitative bond strength measure.

The nominal energy of the shock laser is recorded. With time, the maximum energy output from the laser varies due to component aging. The nominal energy value is monitored to determine if the variation in energy will influence the bond strength figure of merit. Thus far, no effect has been detected.

The maximum back surface velocity and HEL are recorded to determine if there is a correlation with interface strength with these material characteristics. Unfortunately, there is not enough data to definitively determine if there is a correlation with these recorded characteristics and the cladding-cladding bond strength.

The semi-quantitative value—the LS shot number—of the debond for each specimen will be pictorially depicted on individual drawings that represent the plates and shock locations. The visual representation is useful to highlight possible fabrication variations that can affect interface strength between the test samples and within the test samples. The presentation of the LS shot number in this manner provides insight to effectively ascribe the cause of variations in and between the plates. The data taken from plates A1C168 and 67-1 highlight probable variations due to fabrication, as discussed below.

Table 1 contains the results from the LS testing of the MP-1 fuel plates A1C168 and 108-3. Fig. 6 shows a pictorial representation of the results from the A1C168 and prior vendor specimens. The results from the five vendor fuel plates in Fig. 6(c) indicate that the LS technique is repeatable since most of the LS shot numbers are '3' or 'intact.' Although, there is a single point with significant loss of bond strength in the plate. This may be due to fabrication imperfections. This possibility will be expounded upon in the Discussion Section.

The testing of the INL HIPed frame 67-1 provides insight to how fabrication variation can affect bond strength. The testing of the 67-1 frame was separated into two sections. An INL fuel plate is typically sheared to shape from the center of a frame. The four leftover pieces are called shear drops. Fig. 7 shows the virtual fuel plate

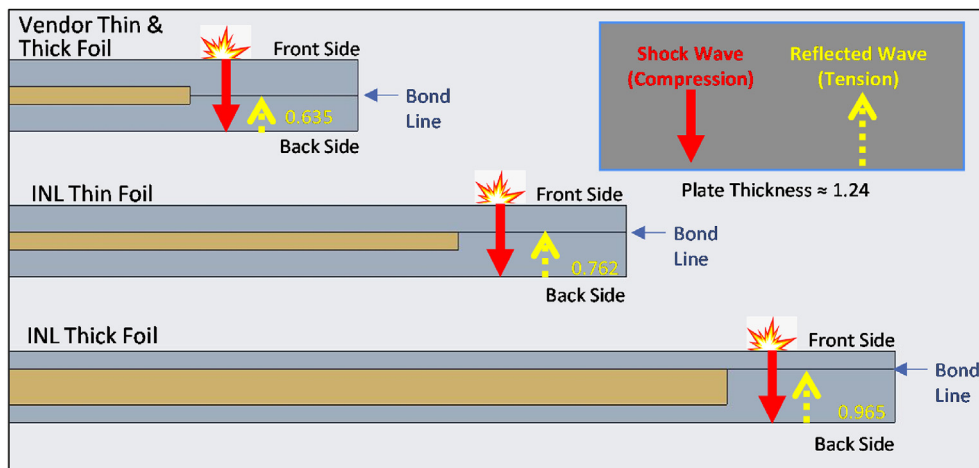
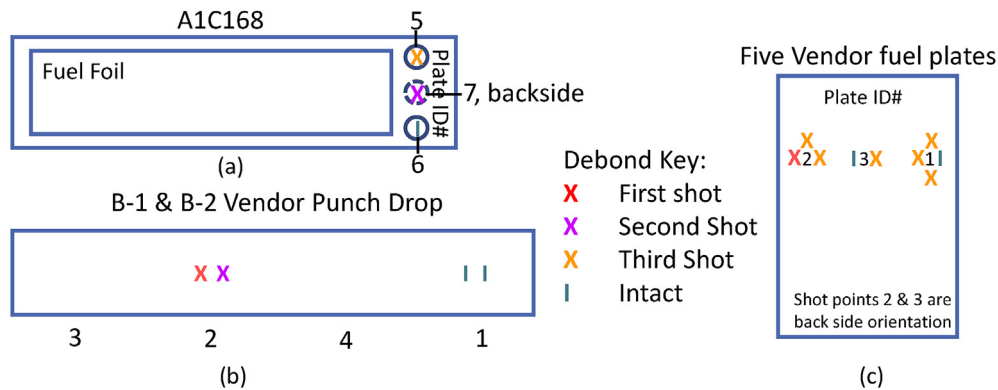


Fig. 5. Schematic diagram that shows the interface locations in the vendor- and INL-fabricated plates for thick and thin fuel foils. Dimensions are in mm.

**Table 1**  
Results from the MP-1 fuel plates (e.g., INL's 108-3 and vendor's A1C168) are presented. The label 'Intact' in the last column indicates that the interface remains unbroken after three full energy shots.

MP-1 Plate Area				
Shot Point	Nominal Laser Energy (J)	1 <sup>st</sup> Shot Velocity (m/s)	1 <sup>st</sup> Shot HEL Velocity (m/s)	Shot Number of Debond
108-3 (asymmetric, thick foil)				
5	2.5	150	20.6	Intact
6	2.5	178.6	20.8	Intact
7 (backside)	2.4	167.2	17.2	1
A1C168 (thin foil)				
5	2.5	190.2	19.4	3
6	2.6	174.4	18.7	Intact
7 (backside)	2.6	168.8	17	2



**Fig. 6.** The pictorial bond strength results for (a) MP-1 plate A1C168 and supporting prior vendor data from (b) the punch drops and (c) fuel plates [19].

roughly centered in the frame, which then defines the shear drop area. Table 2 contains the LS results from the shear drop area of the plate. Table 3 contains the LS results from the virtual fuel plate area. Fig. 7 also shows the pictorial results of the LS testing. The LS shot numbers that cause debonding vary in value from '1' to '3' without an obvious spatial pattern. The bond strength variations found in Fig. 7 may be from normal variations resulting from the fabrication process as most of the LS shot numbers of the plates are '1' and '2.'

The tabular data from INL fuel plate 108-3 was provided previously in Table 1. The pictorial representation shows the results from 108-3 in Fig. 8, in addition to the supplemental results from INL plates A1B106 and A2B104. The data from 108-3 and A2B104 can be directly compared with each other since they both have an inner thick fuel foil, as seen previously in Fig. 5, and the cladding-cladding interfaces are at the same plate depth. The results from shot points 5 and 6 can be directly compared between the two INL thick foil plates. This comparison indicates that 108-3 has a stronger average interface strength since A2B104 shock point 5 failed after one full

power shot. Note that interrogation point 7 in the 108-3 plate is not comparable to points 5 and 6 since point 7 has a backside orientation. The INL interface location is not symmetric with front and back orientation. Since the interface with a backside orientation is closer to the surface that reflects the shockwave, more energy is available to debond the interface since the shockwave attenuation is less. The two thick foil plates indicate that the INL fabrication process shows significant variation between the plates. The results from A1B106 cannot be directly compared with primary plates in this report since the interface is at a different depth within the plate. Unfortunately, this is the only thin plate that was available for testing. The results from the A1B106 thin foil and the 108-3 thick foil do support the assertion that interfaces closer to the far/reflecting surface measures weaker using the LS technique shock points 5 and 6 that failed after the first shot.

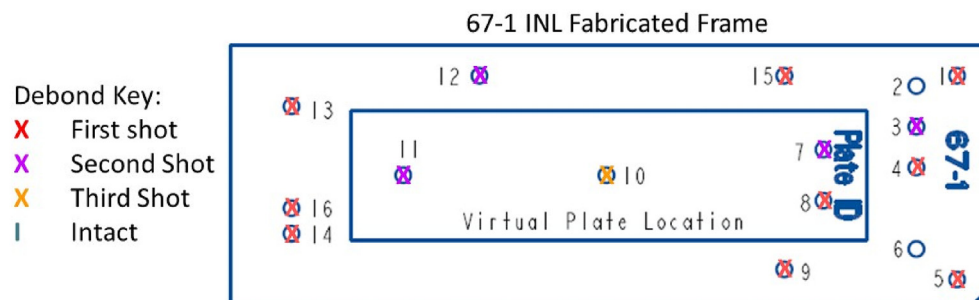


**Fig. 7.** Pictorial bond strength results for frame 67-1, which has been divided into two areas depicting the shear drop and fuel plate interrogation locations.

**Table 2**  
Results from the MP-1 fuel plates (e.g., INL’s 108-3 and vendor’s A1C168) are presented.

67-1 Shear Drop Area				
Shot Point	Nominal Laser Energy (J)	1 <sup>st</sup> Shot Velocity (m/s)	1 <sup>st</sup> Shot HEL Velocity (m/s)	Shot Number of Debond
1 <sup>a</sup>	2.45	176.9	14.3	1
3	2.45	176.1	16.2	2
4 <sup>a</sup>	2.5	161.7	18.7	1
5 <sup>b</sup>	2.4	220	19.2	1
9	2.5	178.3	18.9	1
12	2.35	161.4	15	2
13	2.3	183.4	18.5	1
15	2.7	171.9	13.8	1
14 (1.25 mm)	2.4	174.2	21.9	1
16 (1.24 mm)	2.8	165.9	17.8	1
<b>average</b>	2.48	177	17.4	1.2
<b>STD</b>	.15	16.8	2.6	0.4

<sup>a</sup> Thicker automotive transparent tape was used.  
<sup>b</sup> ‘Extreme’ shockwave amplitude for an unknown reason.

**Table 3**  
Plate 67-1 interrogation results for the LS shot locations within the virtual plate position in the center portion of the frame.

67-1 Virtual Plate Area				
Shot Point	Nominal Laser Energy (J)	1 <sup>st</sup> Shot Velocity (m/s)	1 <sup>st</sup> Shot HEL Velocity (m/s)	Shot Number of Debond
7	2.3	157.5	24.7	2
8	2.4	163.3	19.9	1
10	2.25	171.1	21.1	3
11	2.4	165	20	2
<b>average</b>	2.34	164.2	21.42	2
<b>STD</b>	0.075	5.6	2.25	0.82

**5. Discussion**

For the type of semi-quantitative characterizations being made, the sample population is too small to draw definitive conclusions mostly due to the unknown variability in the test specimens. The results do show definite trends in the data that should be confirmed by additional testing. The data does indicate that the LS characterization technique developed for cladding-cladding interface characterization is reliable and repeatable. The total variability, including plate and LS variability, has been shown to be a change of ‘1’ in the LS shot number. It is very difficult to design tests to separate measurement variations caused by sample variation and instrument variabilities. To separate the measurement uncertainties from the sample fabrication variations, it would require the fabrication of sufficient samples under strict fabrication processes. The fabrication processes would need to be held to tight specifications to provide adequate statistical certainty. In general, the vendor plates nominally measure ‘3’ on the LS shot number scale.

The data shown pictorially in Fig. 6(c) indicate that the LS technique is reliable and the vendor fabrication process, for the most part, is repeatable near the stamped end of the fuel plate. Eight of the LS points for the three interrogation locations in Fig. 6(c) have an LS shot number of ‘3’ or are ‘intact.’ Only one LS point has a debond value of ‘1’ at location 2. The weak value is substantially less than at the rest of the points. This is an indication that this weak location may be caused by a fabrication issue. Since most of the LS interrogation locations broke on the third shot and only two remained intact, the actual interface failure threshold is likely to be close to the LS shot number 3 for typical interfaces. If this is the case, the interface strength difference between 3 shots and intact for vendor plates could be small and within the quantization error of the LS technique.

Fig. 6(b) also suggests that there can be systematic variation in a fabrication process. The B-1 and B-2 vendor punch drop data demonstrates a possible spatial interface strength trend. It should be noted that the pedigree of the vendor punch drops is unknown and the orientation with respect to the stamped end and side of the punched fuel frame are also unknown. The location where the samples were punched out of the vendor frame is given in Fig. 9. The B-1 and B-2 punch drop test locations are shown in Fig. 6(b) and indicate that shot location 1 at the right end of the punch drop has a significantly higher bond strength figure of merit than shot location 2, which is closer to the middle of the two plates.

The INL 108-3 fuel plate has different bond-line geometry as compared to 67–1 and A1C168 as it is an INL thick fuel plate. Plate 108-3 is a good example on how plate geometry affects the measured LS shot number value. The INL plates are fabricated with an asymmetric interface location, as shown in Fig. 5. When the fuel plate has a front side orientation, the interface is closer to the top (e.g., shock) surface. The reflected tensile shockwave has a larger distance to propagate from the bottom (e.g., detection) surface. When the plate has a backside orientation, the interface is close to the bottom side and the reflected shockwave travel distance is small. There is a significant amount of energy absorbed from the shockwave plastically deforming the fuel plate as the shockwave propagates even over short distances (<0.10 mm). Thus, the amount of tensile energy reaching the interface is dependent on the interface depth from the reflected surface.

Plate 108-3 has two LS shot number of intact and one value of ‘1.’ The intact values are for the front side orientation. The measured weak LS shot number at shot point 7 is due to the plate having a backside orientation. Thus, 108-3 has a relatively strong interface strength. The effect of the differences in bond-line location will require modeling to be used to quantitatively compare the fuel plates with different geometries. Useful information can still be

obtained without modeling from 108-3 by qualitatively comparing it to the supplementary plates A2B104 and A1B106. The pictorial results were shown previously in Fig. 8.

The supporting and historical data suggests that the vendor fabrication process is reliable. As shown in Fig. 6(a), vendor plate A1C168 shows typical LS shot numbers of ‘3’ and ‘intact’ in shot points 5 and 6. It should be noted that shot point 7 has a lower LS shot number of ‘2.’ Again, this is most likely a fabrication issue as shot location 7 is the same distance away from the interface. A concern that the center shot point may be weakened by the outer two shot points is not supported by Fig. 6(c). The center shot point location, 3, displays a measured LS shot number of ‘3’ and ‘intact’ in Fig. 6(c).

Since the 67-1 specimen is a blank HIPed frame (e.g., non-fuel), the entire plate is a cladding-cladding interface with a significant amount of area for LS testing. The 67-1 frame provides a unique opportunity to map LS shot number variations within the original HIPed 101.6 mm × 152.4 mm plate prior to shearing out the 25.4 mm × 101.6 mm mini-plate. The LS shot numbers in different areas of the frame can be mapped and compared. The punch drop areas can be compared with the virtual plate area. Fig. 7 shows the LS shot number mapping of the frame 67-1. The measured average for the frame LS shot number is substantially less than the average vendor LS shot number (i.e., ≈ 1.5 vs. ≈ 3). The punch drop area also has a slightly lower LS shot number average than the virtual plate average value (i.e., ≈ 1.2 vs. ≈ 2). The lower LS shot numbers around the frame’s periphery matches the anecdotal experiences. There is no clear pattern seen in the LS shot number map, but it is interesting to note that the ‘strongest’ LS shot number measurement is near the exact center of the frame.

Plate A2B104 has LS shot numbers of ‘1’ and first shot intact. The LS shot number of first shot intact does not offer much information except that the shot point is stronger than the LS shot number of ‘1.’ The LS shot number of one shot in plate A2B104 indicates that shot point 5 is weaker than the stamped end of 108-3. The use of only one full power shot would be useful for a pass/fail qualification test of fuel plates if it could be validated that the LS shot number threshold is sufficient to survive irradiation. The threshold LS shot number would need to be conservatively set by a large margin to ensure the plate’s integrity during irradiation since plate failure in a reactor is not acceptable.

Useful information can also be obtained from comparing the 108-3 thick foil with the A1B106 thin foil. The backside shock orientation for the 108-3 measures weaker than the front side orientation. Testing of the A1B106 thin foil plate also supports the theory that bond-line location makes a difference. From Fig. 5, the thin foil interface is closer to the bottom wall than the thick foil interface by 0.20 mm. Both interrogation locations 5 and 6 in the

A1B106 have a measured LS shot number of ‘1’ with a closer interface to the bottom surface while 108-3 has two LS shot numbers of ‘intact’ with a farther interface. The lower LS shot numbers measured in A1B106 does not mean that the actual interface strength is lower, it just means that the tensile shockwave energy reaching the interface is larger since the thin foil interface is closer to the reflecting (e.g., detection) surface. Again, modeling is needed to directly compare interface strengths in plates with different bond-line geometries.

Testing of plates 108–3 and A1B106 indicate that the tensile amplitude of the shockwave plays a part in causing interface failure in conjunction with the number of shock interrogations. This is an intuitive observation. The implication is that the shock energy can be customized to optimize the energy level to provide a more precise bond strength figure of merit measurement and perhaps increase the number of quantization levels. The cladding-cladding bond strength characterization technique could be modified to measure plates with higher fidelity. The goal would be to lower the laser power and be able to hit the specimen surface more times before the containment layer loses effectiveness. The laser energy would need to be adjusted such that the typical specimen debonds on the last effective shot capable of generating a large amplitude shockwave. The number of effective laser shocks are limited since the LS containment system loses efficacy with each shot. A lower energy pulse may allow an increase in the number of effective LS shots, which would increase the resolution of the bond strength figure of merit and range. Ramping the LS energy to provide better bond strength resolution did not produce consistent results. The interpretation of the results is complicated by the inability to consistently fail the interface with a single high energy shock and the potential variability of bond strength even between closely space interrogation locations.

Just because a plate measures higher on the LS shot number scale does not necessarily mean that the actual bond strength is also higher. The data and shockwave propagation theory thus far indicates that interface depth has a significant effect on bond strength measurements. Table 4 demonstrates the complexity of determining the relative strengths of interfaces with different geometries. The nominal bond strength figure of merit is measured by the average of the number of full power shots it takes to debond the plate’s interface. The estimated actual interface strength order attempts to take plate geometry into consideration. There is high confidence that the vendor sample has the highest actual interface strength, since it has a high LS shot number value of ‘3’ despite the bond-line being the closest to the bottom surface. This indicates that the vendor interfaces are substantially stronger than the INL plates as suggested by the 67-1 results. Plate 67-1 probably has the second highest actual interface strength despite having a low LS

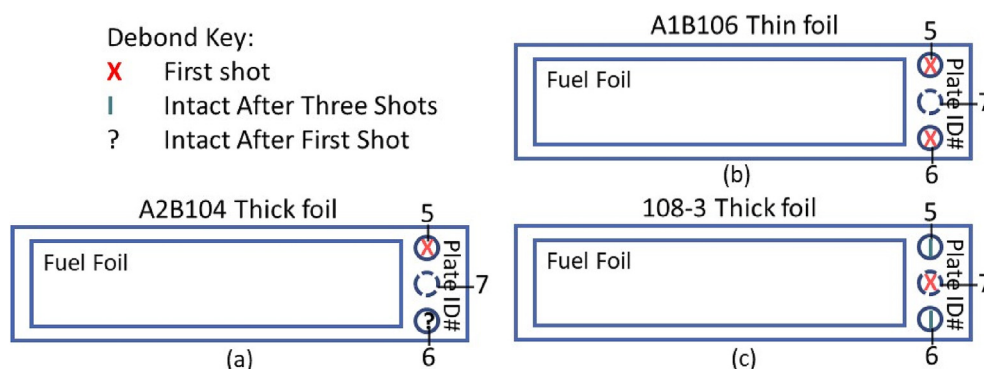


Fig. 8. Pictorial results from prior supplementary INL fuel plates (a) A2B104 and (b) A1B106, as well as (c) primary INL fuel plate 108-3, are displayed for comparison.



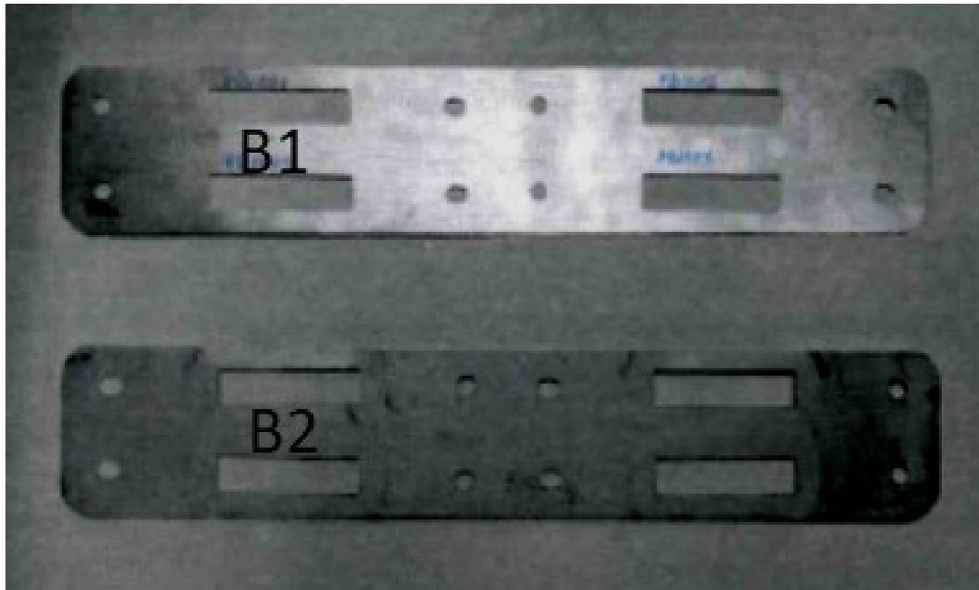


Fig. 9. Punch drops came from vendor HIPed frame locations B-1 and B-2. Vendor frames generating the punch drops have no fabrication pedigree.

Table 4

Geometry complicates the determination of the bond strength figure of merit order, but A1C168 and 67-1 orders have high confidence.

MP-1 Plate Area			
Plate	Interface Depth from Reflecting Surface	LS Shot Number	Bond Strength Ranking 1 = Strongest 4 = Weakest
108-3 (thick, backside)	0.011	1	3
Vendor A1C168	0.025	3	1
67-1 (no foil)	0.025	1.3	2
A1B106 (thin)	0.03	1	4
108-3 (thick)	0.038	Intact	3

shot number value since it is close to the reflecting surface of the plate. The front orientation of plate 108-3 rates low for actual interface strength despite having the highest LS shot number because the interface is farthest from the reflecting surface. As seen in Table 4, the backside orientation for 108-3 brings the measured value down to the lowest value of ‘1.’ The geometry effects are too complicated to have confidence in the interface strength order for A1B106 and 108-3. The LS modeling under development should ultimately be capable of providing a robust bond strength order, as well as quantitative bond strength stress values.

The punch and virtual shear drop samples are from the vendor frame, as shown in Fig. 9, and the INL frame, as shown previously in Fig. 7. Since the fuel plates are cut out of these frames, the LS shot number in the resulting strips should reflect the interface strength of the resulting fuel plates. If the punch and shear drops reliably predict the bond strength in the plate, they can be used in part to qualify the fuel plate. Figs. 6 and 7 pictorially show the LS shot number results from the punch and shear drops. In general, the punch and shear drops tend to measure lower in LS shot number than the fuel plates. The vendor punch drop data in Fig. 6(b) appears to indicate a strength gradient in the fuel plate. The right side of the vendor punch drop is shown to be stronger than the middle of the punch drop. INL plate 67-1 shows consistent measurements in the shear drop areas. The LS shot number average of the shear drop area is lower than the LS shot number in the plate area of the frame. While initial results suggest that the areas outside the fuel plate region have a lower LS shot number, the punch/shear drops may be used as conservative threshold checks for plate qualification. If the punch/shear drop areas pass a minimum threshold LS

shot number value, then the fuel plate should be assured a higher average bond strength. Care must be taken as there can be significant and unexpected loss in localized bond strength caused by the fabrication process.

### 6. Summary/conclusions

The typical cladding-cladding interface in a HIPed fuel plate requires a vast amount of energy to cause interface failure. The amount of energy that it takes to consistently fail a typical cladding-cladding interface is too large for the LSS to provide in a single shot. Thus, a unique cladding-cladding interface characterization technique has been developed. The LS cladding-cladding characterization technique uses full energy laser shots to interrogate the cumulative damage required to break the bond in the cladding areas of the fuel plates. The LS technique for cladding-cladding interfaces provides a semi-quantitative measure of interface strength. The cumulative damage measurement is reported in terms of the number of full energy shots—LS shot number—it takes to generate a debond. The interface depth has been shown to confound the LSS measurement for asymmetric INL plates that were tested with front and back orientations. The LS modeling under development is needed to provide direct correlation to stress and allow for direct comparison between plates with different geometries. Plates with identical geometries and material composition can be directly compared.

Despite the quasi-quantitative characterization technique, the resulting mapping/imaging of bond strength provides effective interface characterization. Since only up to three LS shots can be

effectively executed at one location, the resulting 'quantization' error is relatively large. Despite the quantization limitations, the resulting data are useful in characterizing bond strength throughout the plate. The cladding-cladding characterization technique has been shown to make repeatable characterizations, as well as indicate unexpected weak bond strength locations that could be due to fabrication process imperfections. The total measurement variability of the characterization technique including fabrication and LSS variability is '1' in terms of the reported LS shot number. From the data conveyed in this report, total variation in the bond strength measurements in the vendor and INL samples are equivalent, but the vendor plates are stronger. Currently the LS shot number variability is considerable. We anticipate that with additional research, the measurement variability can be significantly reduced.

The reason that the LS technique is reliable stems from the fundamental physics that are the basis of the technique. A well-defined quantity of energy in the form of a shockwave is input into the fuel plate. The compressive shockwave propagates to the bottom side of the plate. The reflected energy from the plate bottom is in the form of a tensile shockwave, which stresses the interface by trying to pull the interface apart. Fortunately, the interface failure determination is binary. The ultrasonic C-scan does an excellent job of imaging and identifying interface failures. Given that robust cladding-cladding bonds require an astonishing amount of energy to debond, it takes several full energy LS shots at the same location to break most of the interfaces tested with the current LS system.

From LS characterizations of the vendor and INL plates, the results indicate the vendor fabrication process produces fuel plates with stronger LS shot numbers:  $\approx 3$  for the vendor and  $\approx 1.5$  for INL. In general, the vendor plates measure stronger than the INL plates do. The INL shear drop areas also have a slightly lower LS shot number average (e.g.,  $\approx 1.2$ ) than the virtual fuel plate average (e.g.,  $\approx 2$ ). The vendor shear drops also showed weaker locations. Since the LS characterization technique is destructive, the shear drops need to be used to predict the average bond strength figure of merit for the fuel plate where they came from. The shear and punch drop areas in the INL and vendor plates have been shown to have a lower bond strength figure of merit than the actual fuel plate. This behavior is typical of edge effects resulting from fabrication processes. The shear or punch drops would provide a conservative bond strength figure of merit threshold for the corresponding fuel plate.

The different INL fabrication processes show measurable bond strength variation between process runs. INL plate 108-3, which was fabricated after the MP-1 fabrication runs, has a stronger bond strength than the INL MP-1 plate A2B104. INL frame 67-1 was fabricated in a similar manner as the fuel plates irradiated in the successful RERTR-12 irradiation experiment that had no fuel breaching in the plates. There is one significant difference: 67-1 is a center bonded plate since it did not contain a fuel foil. If one assumes that the interface depth has no influence on interface strength during fabrication, an argument can be made that the minimum measured LS shot number in 67-1 is a valid estimate of an insertion threshold for ATR experiments.

Until a larger study can be conducted, it cannot be determined if the strength variations are from variations/differences within the plates, plate positions within a HIP run, or even between HIP runs. From previous testing [18], it was found that within the HIP can, frame position 5 (out of 6) for runs 105, 106, and 107 produced significantly stronger cladding-cladding bond strengths. These research questions and more can be addressed by bond strength testing. The beauty of the LS technique is that the LSS has the ability to answer questions of importance to fuel designers.

The cladding-cladding LS technique can also be used to measure and characterize irradiated fuel plates, as well as fresh fuel plates. Thus, the LS technique can be used to track the performance evolution from fabrication (e.g., sister plates and plate shear drops) to final irradiation. The performance evolution can be monitored and mapped for different areas of the plate. This will allow the plate fabricator to understand the process effects and process changes on the bond strength for fresh and irradiated fuels. This will ultimately lead to a better bond strength threshold that will be determined from punch drops for fuel plate insertion. LSS will enable a fuel qualification specification to replace or supplement the current bend testing of punch drops. A simple production pass/fail test can be used as a qualification threshold in the cladding-cladding region by checking that the interface survives a single full energy LS shot.

The ability of the LS technique to make local measurements and map the bond strength is a unique and valuable capability. The LS technique has found locations in both the vendor and INL plates that have significantly weaker bond strengths despite being surrounded by high bond strength locations. Thus, the LS technique can highlight process variations within a plate and between plates.

### Declaration of competing interest

The authors declare that they have no known competing financial interests or personal relationships that could have appeared to influence the work reported in this paper.

### Acknowledgments

This work was supported by DOE Idaho Operations Office Contract DE-AC07-05ID14517. Accordingly, the U.S. Government retains and the publisher, by accepting the article for publication, acknowledges that the U.S. Government retains a nonexclusive, paid-up, irrevocable, worldwide license to publish or reproduce the published form of this manuscript or allow others to do so, for U.S. Government purposes.

This information was prepared as an account of work sponsored by an agency of the U.S. Government. Neither the U.S. Government nor any agency thereof, nor any of their employees, makes any warranty, express or implied, or assumes any legal liability or responsibility for the accuracy, completeness, or usefulness of any information, apparatus, product, or process disclosed, or represents that its use would not infringe privately owned rights. References herein to any specific commercial product, process, or service by trade name, trademark, manufacturer, or otherwise, does not necessarily constitute or imply its endorsement, recommendation, or favoring by the U.S. Government or any agency thereof. The views and opinions of authors expressed herein do not necessarily state or reflect those of the U.S. Government or any agency thereof.

### Appendix A. Supplementary data

Supplementary data to this article can be found online at <https://doi.org/10.1016/j.net.2022.09.031>.

### References

- [1] Pacific Northwest National Laboratory, Global Threat Reduction Initiative (GTRI) PNNL Convert Program Management Plan, April 2013. PNNL-2243. 2013. Available: [https://www.pnnl.gov/main/publications/external/technical\\_reports/PNNL-22443.pdf](https://www.pnnl.gov/main/publications/external/technical_reports/PNNL-22443.pdf). (Accessed 16 March 2022).
- [2] J.A. Smith, M. Choquet, D. Lévesque, Design of a laser shock system for a remote nuclear radiation environment, in: S.D. Holland, L.J. Bond (Eds.), *AIP Conference Proceedings*, 2102, 2019, 060002.
- [3] J.A. Smith, C.L. Scott, B.C. Benefiel, B.H. Rabin, Interface characterization within a nuclear fuel plate, *Appl. Sci.* 9 (2019) 249.
- [4] M. Perton, D. Lévesque, J.-P. Monchalain, M. Lord, J.A. Smith, B.H. Rabin, *Laser*

- shockwave technique for characterization of nuclear fuel plate interfaces, in: D.O. Thompson, D.E. Chimenti (Eds.), *Review of Progress in Quantitative Nondestructive Evaluation 32*, American Institute of Physics, Melville, NY, USA, 2013, pp. 345–352.
- [5] J.M. Lacy, J.A. Smith, B.H. Rabin, Developing a laser shockwave model for characterizing diffusion bonded interfaces, in: D.E. Chimenti, L.J. Bond (Eds.), *Review of Progress in Quantitative Nondestructive Evaluation 34*, American Institute of Physics, Melville, NY, USA, 2014, pp. 1376–1385.
- [6] J.A. Smith, J.M. Lacy, D. Lévesque, J.-P. Monchalain, M. Lord, Use of the Hugoniot elastic limit in laser shockwave experiments to relate velocity measurements, in: D.E. Chimenti, L.J. Bond (Eds.), *AIP Conference Proceedings 1706*, 2016, 080005.
- [7] J.A. Smith, J.M. Lacy, C.L. Scott, B.C. Benefiel, D. Lévesque, J.-P. Monchalain, M. Lord, in: D.E. Chimenti, L.J. Bond (Eds.), *Further Investigation of Surface Velocity Measurements for Material Characterization in Laser Shockwave Experiments*, vol. 2018, AIP Conference Proceedings, 1949, 180001.
- [8] J.L. Vossen, Measurements of film–substrate bond strength by laser spallation, *ASTM Spec. Tech. Publ. Am. Soc. Test. Mater.* 640 (1978) 122–133.
- [9] V. Gupta, A.S. Argon, Measurement of interface strength by laser-pulse-induced spallation, *Mater. Sci. Eng. A* 126 (1990) (1990) 105–117.
- [10] J. Yuan, V. Gupta, Measurement of interface strength by the modified laser spallation technique: I. Experiment and simulation of the spallation process, *J. Appl. Phys.* 74 (1993) 2388–2397.
- [11] J. Yuan, V. Gupta, A. Pronin, Measurement of interface strength by the modified laser spallation technique: III. Experimental optimization of the stress pulse, *J. Appl. Phys.* 74 (1993) 2405–5107.
- [12] C. Bolis, L. Berthe, M. Boustie, M. Arrigoni, S. Barradas, M. Jeandin, Physical approach to adhesion testing using laser-driven shock waves, *J. Phys. D: Appl. Phys.* 40 (2007) 3155–3163.
- [13] M. Arrigoni, S. Barradas, M. Braccini, M. Dupeux, M. Jeandin, M. Boustie, C. Bolis, L. Berthe, Comparative study of three adhesion tests (EN 582, similar to ASTM C633, LASAT [LASer Adhesion Test], and bulge and blister test) performed on plasma sprayed copper deposited on aluminum 2017 substrates, *J. Adhes. Sci. Technol.* 20 (2006) 471–487.
- [14] V. Gupta, J. Yuan, Measurement of interface strength by the modified laser spallation technique: II. Applications to metal/ceramic interfaces, *J. Appl. Phys.* 74 (1993) 2397–2404.
- [15] Idaho National Laboratory, MP-1 Reference Plates Fabrication Summary Report, Idaho National Laboratory Report INL/LTD-19-55200, 2019.
- [16] Idaho National Laboratory, MP-1 Fabrication at Vendor, Idaho National Laboratory Report SOW-12333, 2018.
- [17] C.R. Clark, J.-F. Jue, G.A. Moore, N.P. Hallinan, B.H. Park, Update on Monolithic Fuel Fabrication Methods, Idaho National Laboratory Report INL/CON-06-11897, October 2006.
- [18] J. Smith, B. Benefiel, C. Scott C, Review of Laser Shock Characterization Results for MP-1 Fresh Fuel Plates, Idaho National Laboratory Report INL/EXT-20-59982, December 2020.